Published in final edited form as:
Expert Rev Med Devices. 2010 May ; 7(3): 343–356. doi:10.1586/erd.10.14.

Laser direct writing of micro- and nano-scale medical devices

Shaun D Gittard[1] and **Roger J Narayan**[1,†]

[1]Joint Department of Biomedical Engineering, University of North Carolina and North Carolina State University. Campus Box 7115, Raleigh, NC 27695-7115, USA

Abstract

Laser-based direct writing of materials has undergone significant development in recent years. The ability to modify a variety of materials at small length scales and using short production times provides laser direct writing with unique capabilities for fabrication of medical devices. In many laser-based rapid prototyping methods, microscale and submicroscale structuring of materials is controlled by computer-generated models. Various laser-based direct write methods, including selective laser sintering/melting, laser machining, matrix-assisted pulsed-laser evaporation direct write, stereolithography and two-photon polymerization, are described. Their use in fabrication of microstructured and nanostructured medical devices is discussed. Laser direct writing may be used for processing a wide variety of advanced medical devices, including patient-specific prostheses, drug delivery devices, biosensors, stents and tissue-engineering scaffolds.

Keywords

ablation; laser; MAPLE direct write; medical; rapid prototyping; selective laser sintering; stereolithography; two-photon polymerization

Laser-based fabrication technologies have recently been used to prepare medical devices with microscale and submicroscale features [1,2]. Lasers exhibit several properties that are advantageous for fabrication of medical devices. For example, it is desirable to incorporate biological molecules (e.g., proteins) and cells into materials used in medical devices, including scaffolds for tissue engineering and drug-delivery devices [3,4]. Nanostructured materials may be used to guide the attachment of individual biological molecules with better control, selectivity and sensitivity than conventional microstructured materials. For example, nanostuctured materials may be able to interact with proteins in a manner that does not alter their biological properties [5].

Processes such as fused deposition modeling and wet etching are not suitable for fabricating medical devices containing biological molecules, since biological molecules can be irreversibly damaged by high temperatures and highly acidic or basic pH environments. Laser direct write techniques are commonly used for fabricating medical devices since they

† Author for correspondence: Fax +1 509 696 8481, roger_narayan@unc.edu.

Financial & competing interests disclosure: This material is based upon work supported by the National Science Foundation under Grant No. 0936110. Roger Narayan is principal investigator on grants from the National Science Foundation, the Department of Defense and the National Institutes of Health on laser-based rapid prototyping of medical devices, including devices for transdermal drug delivery and scaffolds for tissue engineering. In addition, he has received financial support from two companies with an interest in laser direct writing technology in the form of contract research and consulting work; this funding was used to support research and prepare expert guidance on the development of novel drug delivery technologies. The authors have no other relevant affiliations or financial involvement with any organization or entity with a financial interest in or financial conflict with the subject matter or materials discussed in the manuscript apart from those disclosed.
No writing assistance was utilized in the production of this manuscript.

do not require harsh chemicals or heating of material. Lasers have been used in the production of a variety of medical devices, including stents, prostheses, medical sensors, drug-delivery devices and tissue-engineering scaffolds. Medical devices and laser-based techniques used to create them will be discussed in this review.

Lasers provide spatially coherent energy, which can be readily focused in order to process materials at the microscale and the sub-microscale [6]. Emission wavelengths vary greatly, depending on the mechanism used for photon generation. Excimer lasers (e.g., ArF, KrF and XeF lasers) and metal vapor lasers (e.g., HeCd lasers) generally operate at UV wavelengths. Numerous solid-state lasers operate over a wide range from UV to infrared. CO_2 lasers operate at infrared wavelengths [6]. Lasers can either operate in continuous wave or pulsed modes. In continuous wave mode, the energy output is constant over time. Pulsed operation enables higher energies to be emitted over short pulses [6]. When pulses are extremely short, as is the case with ultra-short pulse lasers (e.g., Ti:sapphire lasers) that operate in the femtosecond range, nonlinear optical processes such as two-photon absorption can take place [7]. The phenomenon of two-photon absorption allows femtosecond lasers to perform microscale processes and nanoscale processes that are not possible with other types of lasers. For example, femtosecond laser–material interaction is utilized in a direct write technique known as two-photon polymerization (2PP). For additional information on various types of laser systems, the text *Introduction to Laser Technology* by Hitz, Ewing and Hecht is suggested [6].

In laser direct writing, 2D and 3D structures are prepared by directing a laser beam in a desired pattern over a region of a surface. Writing is controlled by translating the laser, translating the target or rotating the target. With three axes of translation and three axes of rotation, up to six degrees of freedom may be achieved. Direct write rapid prototyping exhibits many attributes that are appealing for use in medical device fabrication. One advantage of laser direct writing techniques over other manufacturing techniques, such as molding, is that devices with complex interior geometries can be fabricated in order to precisely meet the needs of a given application. The geometry of a given structure may be determined by an input stereolithography (SLA) file, which can be easily manipulated using standard computer-aided design (CAD) software [8]. Modifications to the geometry of the structure can be readily performed. Over the past two decades, technologies for producing CAD models based on computed tomography (CT), MRI and other medical imaging techniques have been developed [9–14]. Patient-specific medical devices and prostheses may be prepared using CAD models derived from patient data. These patient-specific prostheses may possess suitable features, including geometry, size and weight for a given patient and a given medical condition. Features may be incorporated into customized prostheses in order to promote tissue ingrowth or other types of cell–prosthesis interaction. In addition, a surgeon can use rapid prototyping in order to fabricate an exact replica of a given patient's anatomical features to aid him or her in surgical preparation and training.

Interaction between the near-surface region of a solid material and either a continuous wave laser beam or a pulsed laser beam involves electronic excitation and electronic de-excitation [15–17]. The most important parameter for understanding laser–material interaction is the laser wavelength; the laser wavelength determines the extent of absorption and scattering of laser radiation in the material [16]. For example, laser ablation involves absorption of the laser radiation by the material, which results in conversion of optical energy to heat within a relatively small volume. Parameters of importance for pulsed lasers are the pulse duration (duration of laser emission), the repetition rate, the duration of laser exposure (time the laser is emitting radiation), the pulse energy (amount of energy in one laser pulse), the numerical aperture, the average power (total energy per unit time), the peak power (pulse energy divided by pulse duration) and the fluence (amount of energy delivered to sample surface

per unit area). The parameters of importance for continuous-wave lasers are the power (total energy per unit time), the irradiance (power per unit area), the numerical aperture and the duration of laser exposure (time the laser is emitting radiation).

Absorption of photons can lead to excitation of electrons in atoms and molecules of the target material. In ablation, energy transfer leads to nearly instantaneous release of the target material, either by thermal vaporization or by photochemical interactions [7]. At lower energies, the bonds remain intact and energy is converted into heat [18]. In this case, localized heating of the target material results in sintering or melting. On the other hand, photopolymerization takes place when photoinitiator molecules absorb photons and form radicalized molecules; these radicals can initiate polymerization reactions [19]. Numerous laser direct write techniques have been developed, which utilize these laser–target interactions. A summary of the laser-based direct write techniques is provided in Table 1. Commonly used laser-based direct write techniques include selective laser sintering (SLS), laser ablation machining, matrix-assisted pulsed-laser evaporation direct write (MAPLE DW), SLA and 2PP.

Selective laser sintering/melting

Powder-based direct write techniques involve selective melting of powders or granules in a powder bed using a high-power laser. For example, in selective laser sintering or melting, a laser is used to heat a powder to a temperature at which the particles either sinter together or melt together, respectively [18]. Prior to laser exposure, the precursor material is commonly annealed to a temperature close to its melting point; only a small increase in temperature is required to cause localized melting or sintering. Since this technique is thermally activated, lasers with greater thermal effects, such as continuous wave lasers (e.g., CO_2 lasers) [20] and long pulse lasers [21], are commonly used. Sintering/melting only occurs in a localized region due to the fact that a focused laser beam is used to heat the powder. A three-dimensional structure is fabricated by moving a height-adjustable table, which contains the powder bed. After sintering of a layer has taken place, a fresh layer of powder is applied to the top surface of the structure; this process is repeated until the device is complete. The processing environment is commonly filled with an inert gas in order to minimize oxidation of the powder. Once fabrication is complete, the unsintered/unmelted powder is removed by breaking out methods, such as manual removal, brushing and powder blasting [22]. The technique may be used to fabricate 3D structures with complex features such as overhangs and undercuts. A diagram of the SLS/selective laser melting (SLM) process is provided in Figure 1A.

Structures with 50-μm features are commonly prepared using conventional selective laser sintering/melting methods [23]. Exner *et al.* recently described a process known as laser micro-sintering for processing metallic (e.g., copper, molybdenum and silver) and ceramic (e.g., alumina and silica) powders [24]. This process involved the use of a q-switched solid-state laser (pulse ~200 ns), which provided high fluence, rapid heating and rapid cooling of material. Metal powders, including copper, molybdenum and silver, were sintered under air without oxidation; the absence of oxidation was attributed to vigorous expansion of the gas and/or the plasma plume. Micro laser sintering using a precursor material containing sub-1 μm grains in an oxygen-free atmosphere provided a sinter layer thickness of 1 μm and a structural resolution of 20 μm. Micro laser sintering using a precursor material containing 10 μm grains in an oxygen-free atmosphere provided a sinter layer thickness of 10 μm and a structural resolution of 55–60 μm. Regenfuss *et al.* used a q-switched solid-state laser and a ring rake for processing of submicrometer powders, including Al_2O_3 and SiC; they obtained resolution and surface roughness values more than one order of magnitude better than those achieved by conventional selective laser sintering technologies [25].

Although SLS/SLM is compatible with various materials, the precursor material must be in powder form [21–23,26–31]. A benefit of SLS/SLM is that support structures are not needed for parts with overhangs, since the unaltered powder acts as a support [32]. It is important to note that SLS/SLM not only provides models for examination, but also functional prototypes for testing. It is also important to note that SLS/SLM is the only laser direct write process that is currently available for producing metallic medical devices and prostheses. Dimensional differences between SLS models fabricated from CT data and master structures were recently shown to be 1.79% [33]. Kaim *et al.* recently compared CT data, the resulting SLS model and CT data of the SLS model [34]. The differences between these three data sets were shown to be statistically insignificant (the likelihood of this finding by chance alone is less than 5%), indicating that the limiting factor in CT-based SLS is the resolution of the scanning technique and not the resolution of the fabrication technique. Further corroborating this observation, dimensional errors in CT measurements have been reported to be as high as 2.16% [35]. With the ability to accurately fabricate structures based on CT data, SLS/SLM can be used to produce patient-specific prostheses and other medical devices. Recent studies have demonstrated that nasal and maxillary prosthetics fabricated using SLS/SLM may be implanted into the human body [36,37]. In addition, SLS enabled tissue-engineering scaffolds with 50 μm features to be fabricated. Lohfeld *et al.* and Williams *et al.* have demonstrated the use of SLS in tissue engineering [37,38]. Using micro-CT (μCT) and SLS, Partee *et al.* fabricated structures for use as tissue-engineering scaffolds [39]. Porcine and human condyles were modified to produce models that replicated the geometries of natural bone porous frameworks. These models were subsequently used to create tissue-engineering scaffolds by SLS of polycaprolactone (Figure 1B). *In vivo* studies of tissue-engineering scaffolds prepared using SLS have recently been reported; radiographic studies by Kanczler *et al.* demonstrated that SLS-fabricated polylactic acid scaffolds supported regrowth and bridging of bone gaps in mice [40].

Recent research efforts have focused on performing SLS/SLM with nontoxic biocompatible materials that are used in artificial tissues and medical prostheses. Several materials, including bioactive ceramics, natural materials, thermoplastic polymers, polymer-coated metals and metals have been processed by means of selective laser sintering [21,23,26–31]. Salmoria *et al.* prepared biodegradable starch–cellulose and cellulose acetate scaffolds using selective laser sintering; these scaffolds have potential applications in drug delivery and in bone replacement [41]. SLS/SLM may also be utilized for processing biomedical ceramics, including alumina–zirconium, alumina–silica and PLGA–hydroxyapatite composites, and bioactive glasses [27–31]. Shishkovsky *et al.* processed porous structures using mixtures of aluminum, alumina and/or zirconia powders; these materials are commonly used in medical tools [42]. Zhang *et al.* examined processing of hydroxyapatite-reinforced polyamide and polyethylene composites by means of selective laser sintering [43]. These composites were shown to support normal metabolism and growth of primary human osteoblast cells. Composites containing higher amounts of hydroxyapatite exhibited increased rates of alkaline phosphatase activity, osteocalcin production and cell proliferation. von Wilmowsky *et al.* incorporated nanosized carbon black, b-tricalcium phosphate or bioactive glass 45S5 within polyetheretherketone; cell proliferation on selective laser sintering-processed materials was examined using human osteoblasts [44]. The polyetheretherketone–bioactive glass composites were shown to possess the highest rates of cell proliferation. Hao *et al.* prepared single-layer and multilayer block specimens with composites of high-density polyethylene reinforced with hydroxyapatite by means of selective laser sintering; these materials have possible uses in tissue scaffolds and customized implants [45]. They suggested that the presence of hydroxyapatite particles on the surfaces of the specimens may serve to impart bioactive properties; bioactive properties include enhanced ingrowth of bone into the scaffold, as well as increased formation of bone in the region surrounding the scaffold. Shishkovsky *et al.* examined layer-by-layer synthesis of porous titanium and

nitinol structures using selective laser sintering/melting [46]. Nitinol is a nickel–titanium alloy that exhibits corrosion resistance, superelasticity and shape memory properties; applications for this alloy include use in stents, craniofacial implants and orthodontic devices [46–48]. SLS/SLM was also used for processing titanium–hydroxyapatite and nitinol–hydroxyapatite composites. Shishkovsky *et al.* evaluated the growth of primary cultures of dermal fibroblasts and mesenchymal stromal human cells on these structures; no cytotoxicity was observed. In addition, the histocompatibility of titanium and nitinol implants was demonstrated using a murine model. Tan *et al.* demonstrated that SLS may be utilized with several classes of biomedical polymers, including polyetheretherketone, poly(vinyl alcohol), polycaprolactone and poly(L-lactic acid) [26]. For example, Rimell and Marquis prepared solid linear continuous structures using ultra-high molecular weight polyethylene [49]. In recent work, Schmidt *et al.* created structures with porosities between 0 and 15% out of polyetheretherketone, a semi-crystalline, nonresorbable, corrosion-resistant, thermoplastic polymer that is commonly used in medical implants [50].

The use of SLS/SLM in biomedical applications is limited by several factors. For example, many feedstock materials are heated to temperatures higher than 37°C in order to enable sintering or melting; this requirement eliminates the possibility of incorporating biological materials (e.g., proteins, nucleic acids or living cells) within materials during SLS/SLM processing. On the other hand, several studies have demonstrated that cells can be seeded on materials after SLS/SLM processing [42–44]. Materials processed by SLS generally exhibit high porosities and significant surface roughness, and often have inferior mechanical properties as compared with the bulk material [18,21]. Since SLM involves complete melting of the feedstock material, materials processed using SLM exhibit mechanical properties that are more similar to those of the bulk material [18].

Laser machining

In laser machining, small amounts of material are removed from bulk material by laser ablation. Ablation occurs in the region of photon absorption where fluence is sufficiently great to enable bonds to be broken; the resolution of this process is dependent on the spot size of the laser [51]. The laser energy may be focused using optics in order to decrease the spot size and consequently increase the fluence. By controlling the location of laser–target interaction, small amounts of material are removed from the bulk material and a structure with the desired shape is produced. It is important to note that the target material must absorb energy at the given laser wavelength in order for ablation to occur. In addition, materials that exhibit poor absorption may require additional energy in order to obtain ablation [51]. Since most materials absorb ultraviolet energy, ultraviolet lasers are commonly used. Due to their higher energy densities and smaller spot sizes, pulsed lasers (e.g., excimer lasers) are frequently used for laser machining. Continuous wave lasers (minimum spot size ~50 μm) are used for situations in which high throughput is of greater concern than precision [52,53]. In laser machining, device fabrication is performed by incremental removal of material using a laser. As such, laser machining is limited to ‘line-of-sight’ operations; ablation cannot take place at locations where the laser path is obstructed. This constraint limits the geometries that can be fabricated by laser machining; structures with overhangs or interior geometries generally cannot be produced using this process. It should be noted that micromachining of structures with interior geometries may be performed with a femtosecond laser. Ablation of optically transparent materials with ultra-short pulse lasers occurs at the focal point; as such, structures with interior geometries may be created [1].

Ablation can occur either by thermal or photochemical mechanisms [7]. In thermal ablation, the energy transfer from the laser beam results in rapid heating and vaporization of the target

material [7]. Thermal ablation is often observed with continuous wave lasers; however, it may also be observed with long pulse lasers [53]. Due to the fact that it is associated with higher processing temperatures and larger heat-affected zones, the thermal ablation mechanism is not commonly used for fabrication of medical devices. Photochemical ablation is more commonly used for fabrication of medical devices. When the transferred energy is greater than the bonding energies of the molecules in the target material, photon absorption breaks bonds in the target material. As a result, the material vaporizes with minimal thermal effects [54]. Target materials with high absorption coefficients and low thermal conductivities exhibit better photochemical ablation efficiency rates, since the transfer of laser energy to electron excitation is more efficient [53]. High energies and short pulse durations are desirable laser properties; on the other hand, long pulse durations increase thermal effects. If insufficient laser energy is present, the excited electrons will return to their resting state, resulting in fluorescence; this phenomenon is utilized in medical imaging techniques such as confocal fluorescence microscopy and Förster resonance energy transfer microscopy [51]. Femtosecond lasers may be used for two-photon absorption; this nonlinear laser–material process involves simultaneous absorption of two photons by a material [55]. Two-photon absorption is influenced by several parameters, including laser wavelength, pulse duration, exposure time, repetition rate, numerical aperture of the optics and material properties (e.g., bandgap).

Two-photon absorption may be used for ablation of materials that exhibit poor absorption, such as fused quartz and various glasses [56]. In addition, thermal effects are less pronounced, since energy transfer is confined to a small volume in the vicinity of the laser focus. [7]. Sub-microscale features may be achieved when machining with femtosecond lasers [1,54,56,57].

During machining with long pulses, ablation of material in the liquid phase can occur; this process results in an irregular etch area [7]. Thermal effects are a significant concern in laser machining of materials; melting, cracking, spallation and burr formation may take place [53]. The ablated material in liquid or vapor form may flow away from the laser–material interaction site in a mushroom-shaped plume [58]. Redeposition (the settling of ablated material on the surface) and recasting of material may also take place [58]. These processes are undesirable, since the redeposited material often exhibits a different surface morphology to the unaltered material. Redeposition is commonly observed in ablation of metals [59]. Laser machining under vacuum is one technique that can be used to reduce the redeposition process [60].

Laser machining is commonly used for fabrication of medical devices with microscale features, including vascular stents [61]. Laser machining has been used to fabricate stents using a number of metals, including stainless steel, tantalum, platinum alloys, niobium alloys and cobalt alloys [61]. Self-expanding stents made from shape memory materials (e.g., nickel–titanium alloy) may also be fabricated using laser machining [62]. Machining of stents using lasers involves minimal heating of the stent or alteration of overall stent geometry [62]. In addition, micromachining may be used to fabricate stents from polymeric materials, including resorbable polyesters and other resorbable polymers; pharmacologic agents may be released when the resorbable polymers degrade within the body [54,63,64]. The minimization of thermal effects is a significant consideration for laser processing of polymers and other temperature-sensitive materials. Images of stents prepared by laser micromachining are shown in Figures 2A & 2B. Figure 2A contains a scanning electron micrograph of a stent that was machined using a CO_2 laser; indiscrete edges, melting and other thermal effects suggestive of large heat-affected zones are observed. Melted features, burrs, cracks and other defects created during the laser micromachining process may lead to stent failure [53]. By comparison, a stent prepared by femtosecond ablation (Figure 2B)

demonstrates smooth, discrete edges. Materials processed using ultra-short pulse lasers show fewer thermal effects; for example, an absence of burrs was noted in microscale features processed using a femtosecond laser [63]. Unlike some laser processes that have taken considerable time for translation into clinical use, femtosecond laser machining of stents has been rapidly commercialized.

Laser machining of biocompatible materials has also been used to create scaffolds for tissue engineering. For example, ablation can be used to fabricate scaffolds for tissue engineering with controlled pore size and porosity. Machining can also be used to control cell orientation and location; for example, lasers may be used to fabricate channels in which cells are subsequently seeded [65]. Duncan *et al.* demonstrated the use of laser machining to examine the effects of surface micro-topography on cells [66]. A KrF excimer laser was used to make channels in poly(ethylene terephtalate) with various widths, spacings and depths. Their study found that micro-topography affects the orientation and adhesion of human umbilical endothelial cells. Orientation of human aortic vascular smooth muscle cells was also shown to be modified by laser-machined grooves on silicon substrates [53]. In a recent study by Patz *et al.*, an ArF laser was used to micromachine 60–400 μm diameter channels into 2% agarose surfaces; the surfaces of the channels were subsequently lined with basement membrane matrix solution [67]. They demonstrated differential adherence of C2C12 myoblast-like cells on these structures; the cells aligned parallel to the 60–150 μm channels. Live/dead assays showed that cell size, cell number, as well as number of nuclei per cell, increased over 72 h. Moreover, some of the myoblast-like cells fused into multinucleated myotube structures. Doraiswamy *et al.* performed a similar study involving B35 neuroblast-like cells [68]. The neuroblast-like cells proliferated and formed bundles after 72 h. Electrospun polymers are being considered for use as scaffolds for tissue engineering; laser micromachining may be used in order to improve proliferation of cells within interior regions of these materials [65]. Choi *et al.* demonstrated that femtosecond laser micromachining may be used for microscale structuring of electrospun polycaprolactone nanofiber meshes [69]. They demonstrated that femtosecond laser ablation provided more uniform patterns than q-switched nanosecond laser ablation. Melting of fibers was observed along the edges of grooves; these features were attributed to laser fluences that were lower than the ablation threshold. Laser micromachining may also be used to pattern channels in microfluidic devices. For example, laser-micromachined transparent materials may be incorporated within optical microfluidic sensors in lab-on-chip devices [70,71]. Optical waveguides may allow fluorescence measurements to be obtained within microfluidic devices such as microscale cell sorting devices [70]. Recent work by Ke *et al.* and Kim *et al.* demonstrated the use of femtosecond lasers for producing microfluidic devices; for example, channels with sub-micrometer diameters were fabricated [1,2]. In addition, they demonstrated that femtosecond lasers may be used to fabricate interior channels within microfluidic devices. A nanoscale channel laser machined on the interior of a glass substrate using a femtosecond laser is shown in Figure 2C. These microscale cell culture devices may be used for performing controlled experiments on viable cells in an aqueous environment [72,73]. Recent laser machining studies have involved efforts to lower the cost and improve the rate at which laser micromachining is performed. For example, use of short picosecond lasers for laser micromachining is being examined; these devices provide more rapid machining speeds and lower costs than femtosecond lasers [74]. Ancona *et al.* demonstrated that relatively inexpensive 100-ps microchip laser fiber systems can be used to machine metals such as copper, carbon steel and stainless steel; a thin layer of melted material was observed on the picosecond-laser micromachined structures [75].

MAPLE DW

In MAPLE DW, laser ablation is used to transfer material from one substrate to another. The MAPLE DW system, illustrated in Figure 3A, consists of a laser source, a ribbon, a matrix containing the material to be patterned and a substrate. The matrix is spin-coated onto the optically transparent ribbon, which is typically fabricated out of quartz. A nanosecond excimer laser beam passes through the optically transparent ribbon and ablates the matrix. Upon ablation, the material contained in the matrix is transferred from the ribbon to the substrate.

Matrix-assisted pulsed-laser evaporation direct write was originally designed by the US Naval Research Laboratory for fabrication of electronic devices [76,77]. They subsequently demonstrated that the MAPLE DW process could be used for patterning biological materials, including proteins and cells [78,79]. Laser-based techniques such as MAPLE DW provide several advantages over conventional solvent-based techniques, including inkjet printing and Langmuir–Blodgett dip coating. For example, processing of 3D structures using conventional solvent-based techniques is difficult, since dissolution of previously deposited layers may occur during each processing step. Advantages of MAPLE DW include: enhanced biological material–substrate adhesion; deposition can be performed under ambient conditions; the matrix allows the amount of MAPLE DW-patterned material to be quantitatively determined; and multilayered structures can be prepared using multiple quartz disks. For example, patterns of viable *Escherichia coli* were deposited on glass, nutrient agar and silicon substrates using MAPLE DW. Laser–material interaction or shear forces during the MAPLE DW process did not alter *E. coli* growth; green fluorescent protein expression studies demonstrated that the MAPLE DW-processed cells remained viable. The features obtained in the MAPLE DW-transferred patterns are dependent on several parameters, including the matrix material and laser spot size. If relatively large structures (e.g., cells) are being patterned, the feature size is limited by the dimensions of the transferred material. 10-μm features have been achieved for MAPLE DW patterning of proteins; in this case, the dimensions of the transferred biological material do not provide a limiting factor with regard to feature size [80,81].

The matrix can contain either one or two layers. In the one-layer system, the matrix is a suspension containing the biological material and at least one optically absorbing material. When the absorbing material evaporates during ablation, the biological material is transferred to the substrate. One-layer matrices have been used to create microscale patterns of proteins, bacteria and eukaryotic cells [78–80,82]. Viable cells and many biological molecules may be damaged by UV light–material interaction involving a single matrix layer [80]. In the two-layer approach, a release layer containing an absorbing triazene polymer is placed inbetween the ribbon and the biological material. Ablation of the release layer results in transfer of the biological material to the substrate; laser interaction with biological materials within the matrix is minimized. For example, Doraiswamy *et al.* utilized a two-layer system to fabricate mesoscopic patterns of B35 neuroblasts [83]. An image of neuroblast-like cells deposited using the two-layer approach is presented in Figure 3C. Their results suggest that use of the absorbing polymer release layer may enable transfer of viable cells at low laser fluences.

Matrix-assisted pulsed-laser evaporation direct write may be used to create 2D and 3D cell patterns for tissue engineering, drug discovery and other biomedical applications. Patz *et al.* used MAPLE DW to pattern B35 neuroblast-like cells onto and within polymerized extracellular matrix substrates [84]. They fabricated three-dimensional patterns of B35 neuroblast-like cells by varying transfer energy and extracellular matrix solidification. Quartz disks were utilized for attenuating the laser beam without significantly altering the

laser spot size. 2D and 3D arrays of neuroblast-like cells were created within an extracellular matrix substrate. Neuroblast-like cells were initially deposited using a fluence that enabled deep penetration of the extracellular matrix substrate. Neuroblast-like cell arrays were subsequently deposited directly above the initial cell layer by attenuating the laser beam and lowering the laser fluence. In their study, neuroblast-like cells were transferred to depths of up to 75 μm by varying the fluence emitted from the ArF nanosecond excimer laser source. Confocal microscopy studies demonstrated that MAPLE DW-processed B35 cells extended their axons outward, made axonal connections and formed a three-dimensional neural network within the substrate. Terminal deoxynucleotidyl transferase biotin-dUTP nick-end labeling studies demonstrated that 3% of MAPLE DW-processed B35 cells underwent apoptosis. These results suggest that MAPLE DW may be used for layer-by-layer patterning of cells. Doraiswamy *et al.* demonstrated that MAPLE DW may be used to process microscale patterns of bioceramics, including zirconia and hydroxyapatite; patterns of hydroxyapatite on borosilicate glass deposited by means of MAPLE DW are shown in Figure 3B. They also performed co-deposition of hydroxyapatite, MG 63 osteoblast-like cells and extracellular matrix using MAPLE DW [85]. They demonstrated that the MG 63 osteoblast-like cells remained viable when code-posited with hydroxyapatite and extracellular matrix. Entire viable tissue samples have also been processed using MAPLE DW. For example, Wu *et al.* fabricated tissue microarrays using donor prostate tissue and a gelatin release layer [80]. Several challenges need to be overcome in order to expand the use of MAPLE DW for biomedical applications. For example, materials may fragment during MAPLE DW processing [80]. Several parameters, including ribbon–substrate distance, laser energy, spot size, release layer material and matrix composition, influence MAPLE DW-processed cell viability, MAPLE DW processing efficiency, minimum feature size and other outcomes [80].

Stereolithography

Stereolithography (also commonly known as stereolithography apparatus) relies on the release of free radical molecules upon interaction of photoinitiator molecules with UV light. This process may be used to initiate polymerization of a resin-containing precursor and photoinitiator molecules; resins containing acrylate, epoxy, urethane acrylate or vinyl ether functional groups are typically used [86].

Ultraviolet light is guided over a vat containing the resin in the geometry of the desired pattern. Excitation of photoinitiator molecules, formation of reactive species, generation of free radicals, and polymerization of the resin occurs in the region of laser-resin interaction. Polymerization may occur up to a few micrometers below the surface [19,87]. After a given layer is selectively solidified, the structure is submerged within the resin vat by a depth that is equivalent to the thickness of the polymerized layer. The structure is then recoated with unpolymerized resin in order to enable processing of a subsequent layer. The ultraviolet light exhibits a depth of penetration that exceeds the layer thickness; as a result, overcuring of the previously solidified material and adhesion between layers are obtained. Movement of the Z-height stage controls exposure of the laser to the resin vat. X- and Y-stage movements enable selective solidification of material in a given Z-plane. After fabrication of the desired three-dimensional structure, it is placed in a developing solution that washes away the unpolymerized resin. A post-curing step, which involves exposure to high-intensity UV light for up to 2 h, is performed in order to fully polymerize the material. This process increases the hardness and reduces the toxicity of the material, which is correlated with the presence of residual monomers and oligomers. Post-curing may be used to polymerize entrapped liquid resin; this mechanism enables rapid processing of thick structures [32].

Since photoinitiator molecules interact with ultraviolet light containing relatively low energies, continuous wave lasers are typically used; these devices enable structures to be fabricated with accelerated fabrication times and reduced costs. Systems containing less expensive UV light lamps instead of lasers, in which the light is guided by mirrors or fiber optic devices, have also been developed. For example, Gittard *et al.* used a 1280×1024 pixel Direct Light Projection (DLP) SLA system to fabricate scaphoid and lunate bone prostheses in a layer-by-layer manner (build layer = 50 μm) out of a photoreactive acrylate polymer [88]. Fabrication of the bone prostheses was guided using 3D models, which were prepared from patient computer tomography data. SLA is a widely used laser-based rapid prototyping technology, since it can be performed using low-cost equipment and with relatively rapid fabrication times. Structures with feature sizes of 1.2 μm have been reported; however, most commercial systems provide structures with feature sizes greater than 50 μm [19].

Stereolithography of biodegradable polymers for use as tissue-engineering scaffolds has been described in recent studies [4,89]. For example, Lee *et al.* fabricated three-dimensional scaffolds for tissue engineering containing poly(lactic-co-glycolic acid) microspheres, which incorporated the growth factor bone morphogenetic protein 2 [4]. SLA was used to create scaffolds that contained well-connected and regular pores. Polymer–ceramic composite scaffolds have been created using poly(propylene fumarate)/diethyl fumarate and hydroxyapatite; these materials demonstrated better cell proliferation properties than poly(propylene fumarate)/diethyl fumarate scaffolds [90]. An image of a poly(propylene fumarate)/diethyl fumarate–hydroxyapatite composite scaffold is shown in Figure 4A. SLA does not involve high processing temperatures; therefore, biological materials such as proteins, antimicrobial agents and viable cells may be directly incorporated within structures during the SLA process. This capability is beneficial for tissue engineering and drug discovery applications, in which seeding of cells or biological materials on materials may enable the development of more functional devices. Arcaute *et al.* demonstrated that poly(ethylene glycol)-dimethacrylate may be fabricated into complex structures, including structures with internal channels, using SLA; the layer thickness was shown to be related to energy dosage, poly(ethylene) glycol concentration and photoinitiator concentration [91]. They incorporated dermal fibroblasts within poly(ethylene glycol) that was processed using SLA, and demonstrated cell viability of at least 87%. It should be noted that UV light, monomers, oligomers or photoinitiator molecules may cause damage to deoxyribonucleic acid molecules, cell components or biological materials; these concerns must be addressed before incorporation of cells during the SLA process is translated into clinical use.

It should be noted that SLA-processed materials may undergo distortion and shrinkage. In addition, many SLA-compatible resins exhibit high thermal coefficients of expansion, and as such are unsuitable for use as moulds. To overcome limitations with regard to materials selection, master structures may be fabricated out of SLA-compatible materials; end structures may subsequently be fabricated out of other materials by means of molding. Several clinically implanted prostheses have been prepared using SLA-molding techniques, including auricular, maxillofacial and cranial prostheses [92–99]. An example of a cranial prosthesis fabricated using this technique is shown in Figure 4B. It should be noted that fabrication of structures by the SLA-molding process eliminates two advantages provided by SLA: the ability to minimize fabrication times by directly fabricating functional prostheses and the ability to fabricate prostheses with complex interior geometries. For example, Wurm *et al.* demonstrated that SLA and molding may be used to fabricate cranial implants out of a biocompatible, high-strength carbon fiber-reinforced polymer; these implants may be used for treatment of extensive cranial damage [97]. In their clinical studies, excellent intra-operative correspondence between the implant geometry and the patient anatomy was obtained. Follow-up after an extended period of time (mean time = 3.6 years) revealed good reconstruction of the bony defect, with only a few adverse events, including infection,

allergy and hematoma. To the authors' knowledge, laser direct write SLA has not been used for direct fabrication of an implantable prosthesis at this time. Additional studies are needed in order to develop SLA-compatible materials that are suitable for long-tem implantation. Lee *et al.* examined the use of custom-made poly(methylmethacrylate) cranial prostheses for treatment of large (>100 cm^2) cranial defects; these prostheses were fabricated using a CAD/computer-aided manufacturing process. Their work suggested that CAD/computer-aided manufacturing-fabricated poly(methylmethacrylate) prostheses are an appropriate treatment modality for patients who have no autogenous bone available for treatment [97,98].

Two-photon polymerization

Similar to SLA, 2PP utilizes excitation of photoinitiator molecules to induce chemical reactions between photoinitiator molecules and monomers within a transparent resin. Unlike conventional SLA, which uses single-photon absorption for excitation of photoinitiator molecules, 2PP uses two-photon absorption for excitation of photoinitiator molecules. Near simultaneous absorption of two photons creates a virtual state for several femtoseconds; this type of electronic excitation is similar to excitation by a single photon that possesses a much higher energy [100,101]. This two-photon absorption process exhibits a nonlinear (quadratic) relationship with the incident irradiance. Polymerization occurs in locations where energies exceed the excitation threshold of the photoinitiator [102]. Negligible absorption occurs except in the immediate vicinity of the focal volume. The nonlinearity of two-photon absorption enables excitation of photoinitiator molecules and solidification of material to occur within the diffraction limit [102]. 2PP can achieve significantly higher resolutions than other direct write techniques; structures with minimum feature sizes of 100 nm have previously been achieved [102].

A 2PP system consists of a femtosecond laser, a microscope objective and a translational stage (Figure 5A). A femtosecond laser is utilized for achieving two-photon absorption. Standard microscope objectives are used to focus the laser; altering the numerical aperture of the focusing optics can be used to scale the feature size [103]. It is important to note that the voxel size (and hence the feature size of the polymerized structure) is dependent on the energy distribution, which in turn is controlled by the focusing optics [102]. Since sub-micrometer feature sizes are not necessary for all medical devices, direct writing of large structures using small voxels is often both unnecessary and time-consuming. The ability to process structures with a large range of feature sizes enables both production time and cost to be minimized. 2PP involves either moving the resin with respect to a fixed focal point or moving the focal point within the resin. For example, movement of the resin with respect to the laser beam is commonly accomplished using galvano-mirrors, which scan the beam in the X- and Y-directions, and a piezoelectric stage, which moves the resin in the Z- direction [104,105]. Galvano-mirrors offer more rapid processing times than translational stages [103]. Recent studies have described 2PP using galvano-mirrors with a resolution of approximately 1.2 nm per step, and piezeoelectric stages with a resolution of 0.1 nm [104,105].

Two-photon polymerization provides several advantages over conventional processes for scalable fabrication of small-scale medical devices. Many materials processed using 2PP are widely available and are inexpensive. In addition, many materials are transparent to near-infrared wavelength light, which is commonly used in 2PP [87]. The 2PP process can be set up in a conventional environment that does not contain cleanroom facilities or other specialized equipment [103]. Other techniques that are able to produce structures with similar feature sizes, such as deep reactive ion etching and lithography, electroplating and molding, require dedicated cleanroom-based facilities [106]. This is an important benefit,

since fabrication of a device for clinical use can be performed in close proximity to an operating room or another clinical site.

Many medical applications of 2PP have involved fabrication of structures out of photocurable polymers, as well as organically modified ceramic (Ormocer®) materials. Ormocer materials include urethane- and thioether (meth)-acrylate alkoxysilanes. The inorganic components form inorganic Si–O–Si networks by means of hydrolysis and condensation; these networks serve to limit shrinkage of the material. The interactions between the inorganic and the organic networks in Ormocer® materials provide these materials with chemical stability as well as thermal stability. A variety of 3D microstructured medical devices, including microneedles, small prostheses and scaffolds for tissue engineering, may be fabricated by 2PP. For example, microneedles have been fabricated using 2PP [101,107–109]. These devices, which exhibit lancet, thorn or hypodermic needle shapes, contain at least one dimension that is less than 1 mm in length. By reducing device dimensions and minimizing interaction with dermal nerve endings, pain to the patient and damage at the injection site may be reduced [110,111]. Solid microneedles may be utilized in a similar manner to conventional transdermal patches. Hollow microneedles may enable diffusion- or pressure-driven delivery of pharmacologic agents through the needle bore to be adjusted over time. An example of an Ormocer microneedle fabricated by 2PP is provided in Figure 5B. Ovsianikov *et al.* fabricated arrays of in-plane and out-of-plane hollow microneedles with lengths of 800 μm, microneedle base diameters between 150 μm and 300 μm and various aspect ratios [109]. Compression load studies demonstrated that the microneedle arrays penetrated cadaveric porcine adipose tissue without fracture. Human epidermal keratinocyte viability on the Ormocer surfaces created using 2PP was similar to that on control surfaces.

Small bone prostheses are another class of medical devices that have also been fabricated using 2PP. Ovsianikov *et al.* demonstrated fabrication of total ossicular replacement prostheses [103]. Total ossicular replacement prostheses prepared using conventional materials (e.g., Teflon®, titanium and Ceravital®) have demonstrated migration, perforation of the tympanic membrane, difficulty in shaping the prostheses and reactivity with the surrounding tissues. An Ormocer prosthesis was inserted and removed from the intended site of use in a frozen human head without fracture. Prosthesis dimensions can readily be manipulated to conform to patient anatomy [103]. Tissue-engineering scaffolds with unique geometries have also been created using 2PP [112–115]. For example, Doraiswamy *et al.* fabricated Lego®-like interlocking scaffolds using 2PP; attachment of B35 neuroblast-like cells was observed on the raised portions of these structures [101]. A tissue-engineering scaffold containing several pore sizes is shown in Figure 5C. Scaffolds containing several pore sizes may exhibit dissimilar transport rates for cells, nutrients, waste molecules, growth factors and other biological molecules [110]. For example, migration of cells may be limited, while transport of biological molecules may be enabled in these structures. This principle was recently demonstrated by Tayalia *et al.*; scaffolds were fabricated with pore sizes ranging from 12 to 110 μm. Cells were able to penetrate scaffolds with larger pores, but were not able to penetrate scaffolds with smaller pores [113]. 2PP has been used to process scaffolds out of several materials, including Ormocer, poly(ethylene glycol) diacrylate, triacrylate and polycaprolactone-based tri-block copolymers [100,101,110,113,114]. Unlike other laser direct write methods, 2PP may also be used to fabricate structures with submicrometer features (e.g., structures on the same length scale as subcellular organelles).

Key issues

- Thermal effects are of concern for laser-based processes, such as selective laser sintering/melting and laser machining. Thermal effects such as melting, burr formation and cracking may limit the function of laser-fabricated structures.
- Resolution tolerances must be optimized in order to maximize efficiency. Structures with larger features may exhibit inferior performance; however, fabrication of structures with smaller features involves longer fabrication times and higher fabrication costs.
- There are currently a limited number of materials that are compatible with each laser direct write technique. The development of novel organic and inorganic precursor materials will enable wider use of laser direct write technologies.
- The effects of laser–biological material interaction (e.g., heat, UV light–biological material interaction, photoinitiator–biological material interaction) must be more fully evaluated.
- Degradation of laser direct write-processed materials has not been fully evaluated. Studies are needed to examine biological, chemical, corrosion and mechanical properties of the resins, breakdown products and diluents used in laser direct write techniques.

Expert commentary

Over the past decade, significant advances have taken place in the field of laser direct writing. For example, two direct write processes, MAPLE DW and 2PP have been developed over the past decade. Other techniques have benefited from decreases in minimum feature size and improvements in materials selection. Laser direct write techniques have recently been used for fabrication of prostheses, scaffolds for tissue engineering and other advanced medical devices. Reductions in the minimal feature sizes offered by various laser direct write techniques will expand the number of potential medical applications. In addition, laser direct write technologies will benefit from a wider selection of materials. The development of laser direct write-compatible materials with improved biological, chemical, corrosion and mechanical properties will enable laser direct write technologies to be used in a greater number of medical applications.

Five-year view

Proof-of-concept studies have been completed for many laser direct write technologies. Over the next several years, detailed *in vitro*, *in vivo* and clinical studies of patient-specific prostheses and other medical devices will be completed. Ultra-short pulse lasers will likely see more frequent use in laser direct writing due to their ability to fabricate devices with smaller features and devices with interior geometries. Advances in tissue engineering and in medical devices could result from the development of structures with both microscale and submicroscale features. In the near future, significant advances in microstructured and nanostructured medical devices will take place as a result of improvements in laser devices, computational methods and biomaterials.

References

Papers of special note have been highlighted as:

• of interest

•• of considerable interest

1. Ke K, Hasselbrink EF, Hunt AJ. Rapidly prototyped three-dimensional nanofluidic channel networks in glass substrates. Anal Chem 2005;77(16):5083–5088. [PubMed: 16097742]
2. Kim TN, Campbell K, Groisman A, Kleinfeld D, Schaffer CB. Femtosecond laser-drilled capillary integrated into a microfluidic device. Appl Phys Lett 2005;86(20):201106.
3. Harris ML, Doraiswamy A, Narayan RJ, Patz TM, Chrisey DB. Recent progress in CAD/CAM laser direct-writing of biomaterials. Mater Sci Eng C 2008;28(3):359–365.•Recent report of the progress of matrix-assisted pulsed-laser evaporation direct write technology.
4. Lee JW, Nguyen TA, Kang KS, Seol Y, Cho D. Development of a growth factor-embedded scaffold with controllable pore size and distribution using micro-stereolithography. Tissue Eng A 2008;14(5):835.
5. Lee, KB.; Solanki, A.; Kim, JD.; Jung, J. Nanomedicine: dynamic integration of nanotechnology with biomaterials science. In: Zhang, M.; Xi, N., editors. In Nanomedicine: A Systems Engineering Approach. Pan Stanford; Singapore: 2009. p. 1-38.
6. Hitz, B.; Ewing, JJ.; Hecht, J. Introduction to Laser Technology. 3rd. IEEE Press; New York, NY, USA: 2001. ••Excellent book covering many aspects of laser technology.
7. Liu X, Du D, Mourou G. Laser ablation and micromachining with ultrashort laser pulses. IEEE J Quant Electron 1997;33(10):1706–1716.••Thorough discussion of the physics of ablation with ultra-short pulsed lasers.
8. Han J, Jia Y. CT image processing and medical rapid prototyping. Proc 2008 Int Conf Biomed Eng Informatics 2008;2:67–71.
9. Solar P, Ulm C, Lill W, et al. Precision of three-dimensional CT-assisted model production in the maxillofacial area. Eur Radiol 1992;2(5):473–477.
10. Ellis DS, Toth BA, Stewart WB. Temporoparietal fascial flap for orbital and eyelid reconstruction. Plast Reconstr Surg 1992;89(4):606–612. [PubMed: 1546071]
11. Klein HM, Schneider W, Alzen G, Voy ED, Gunther RW. Pediatric craniofacial surgery – comparison of milling and stereolithography for 3D-model manufacturing. Pediatr Radiol 1992;22(6):458–460. [PubMed: 1437375]
12. Ono I, Gunji H, Kaneko F, Numazawa S, Kodama N, Yoza S. Treatment of extensive cranial bone defects using computer-designed hydroxyapatite ceramics and periosteal flaps. Plast Reconstr Surg 1993;92(5):819–830. [PubMed: 8415963]
13. Eufinger H, Wehmoller M, Machtens E, Heuser L, Harders A, Kruse D. Reconstruction of craniofacial bone defects with individual alloplastic implants based on CAD/CAM-manipulated CT-data. J Craniomaxillofac Surg 1995;23(3):175–181. [PubMed: 7673445]
14. McGurk M, Amis AA, Potamianos P, Goodger NM. Rapid prototyping techniques for anatomical modelling in medicine. Ann R Coll Surg Engl 1997;79(3):169–174. [PubMed: 9196336]
15. Majumdar JD, Manna I. Laser processing of materials. Sadhana 2003;28(3&4):495–562.
16. Jansen ED, Frenz M, Kadipasaoglu KA, et al. Laser-tissue interaction during transmyocardial laser revascularization. Ann Thorac Surg 1997;63(3):640–647. [PubMed: 9066377]
17. Malinauskas M, Gilbergs H, Žukauskas A, Purlys V, Paipulas D, Gadonas R. A femtosecond laser-induced two-photon photopolymerization technique for structuring microlenses. J Opt 2010;12(3): 035204.
18. Kruth JP, Mercelis P, Van Vaerenbergh J, Froyen L, Rombouts M. Binding mechanisms in selective laser sintering and selective laser melting. Rapid Prototyping J 2005;11(1):26–36.
19. Zhang X, Jiang XN, Sun C. Micro-stereolithography of polymeric and ceramic microstructures. Sens Actuator A 1999;77(2):149–156.
20. Antonov EN, Bagratashvili VN, Whitaker MJ, et al. Three-dimensional bioactive and biodegradable scaffolds fabricated by surface-selective laser sintering. Adv Mater Deerfield 2004;17(3):327–330. [PubMed: 17464361]
21. Kathuria YP. Microstructuring by selective laser sintering of metallic powder. Surf Coat Technol 1999;116:643–647.

22. Berry E, Brown JM, Connell M, et al. Preliminary experience with medical applications of rapid prototyping by selective laser sintering. Med Eng Phys 1997;19(1):90–96. [PubMed: 9140877]
23. Wendel B, Rietzel D, Kuehnlein F, Feulner R, Huelder G, Schmachtenberg E. Additive processing of polymers. Macromol Mater Eng 2008;293(10):799–809.•Recent review of additive rapid prototyping techniques, including stereo lithography and selective laser sintering.
24. Exner, H.; Horn, M.; Streek, A.; Regenfuss, P.; Ullmann, F.; Ebert, R. Laser micro sintering – a new method to generate metal and ceramic parts of high resolution with sub-micrometer powder. In: Bartolo, PJ.; Mateus, AJ.; Batista, FDC., et al., editors. Virtual and Rapid Manufacturing – Advanced Research in Virtual and Rapid Prototyping. Routledge; London, UK: 2008. p. 491-499.
25. Regenfuss P, Streek A, Hartwig L, et al. Principles of laser micro sintering. Rapid Prototyping J 2007;13(4):204–212.
26. Tan KH, Chua CK, Leong KF, et al. Selective laser sintering of biocompatible polymers for applications in tissue engineering. Biomed Mater Eng 2005;15(1–2):113–124. [PubMed: 15623935]
27. Shishkovsky I, Yadroitsev I, Bertrand P, Smurov I. Alumina-zirconium ceramics synthesis by selective laser sintering/melting. Appl Surf Sci 2007;254(4):966–970.
28. Gahler A, Heinrich JG, Guenster J. Direct laser sintering of Al_2O_3 – SiO_2 dental ceramic components by layer-wise slurry deposition. J Am Ceram Soc 2006;89(10):3076–3080.
29. Simpson RL, Wiria FE, Amis AA, et al. Development of a 95/5 poly(l-lactide-co-glycolide)/ hydroxylapatite and β-tricalcium phosphate scaffold as bone replacement material via selective laser sintering. J Biomed Mater Res B 2008;84B(1):17–25.
30. Lorrison JC, Dalgarno KW, Wood DJ. Processing of an apatite-mullite glass-ceramic and an hydroxyapatite/phosphate glass composite by selective laser sintering. J Mater Sci Mater Med 2005;16(8):775–781. [PubMed: 15965749]
31. Dyson JA, Genever PG, Dalgarno KW, Wood DJ. Development of custom-built bone scaffolds using mesenchymal stem cells and apatite-wollastonite glass-ceramics. Tissue Eng 2007;13(12): 2891–2901. [PubMed: 17764401]
32. Steen, WM. Laser Material Processing. 3rd. Springer; Berlin, Germany: 2003. Rapid prototyping and low volume manufacture; p. 279-300.
33. Ibrahim D, Broilo TL, Heitz C, et al. Dimensional error of selective laser sintering, three-dimensional printing and PolyJet™ models in the reproduction of mandibular anatomy. J Craniomaxillofac Surg 2009;37(3):167–173. [PubMed: 19056288]
34. Kaim AH, Kirsch EC, Alder P, Bucher P, Hammer B. Preoperative accuracy of selective laser sintering (SLS) in craniofacial 3D modeling: comparison with patient CT data. Rofo 2009;181(7): 644–651. [PubMed: 19253203]
35. Asaumi J, Kawai N, Honda Y, et al. Comparison of three-dimensional computed tomography with rapid prototype models in the management of coronoid hyperplasia. Dentomaxillofac Radiol 2001;30(6):330–335. [PubMed: 11641732]
36. Wu G, Zhou B, Bi Y, Zhao Y. Selective laser sintering technology for customized fabrication of facial prostheses. J Prosthet Dent 2008;100(1):56–60. [PubMed: 18589076]
37. Lohfeld S, McHugh P, Serban D, Boyle D, O'Donnell G, Peckitt N. Engineering Assisted Surgery™: a route for digital design and manufacturing of customised maxillofacial implants. J Mater Process Technol 2007;183(2–3):333–338.
38. Williams JM, Adewunmi A, Schek RM, et al. Bone tissue engineering using polycaprolactone scaffolds fabricated via selective laser sintering. Biomaterials 2005;26(23):4817–4827. [PubMed: 15763261]
39. Partee B, Hollister SJ, Das S. Selective laser sintering process optimization for layered manufacturing of CAPA® 6501 polycaprolactone bone tissue engineering scaffolds. J Manuf Sci Eng Trans 2006;128(2):531–540.
40. Kanczler JM, Mirmalek-Sani S, Hanley NA, et al. Biocompatibility and osteogenic potential of human fetal femur-derived cells on surface selective laser sintered scaffolds. Acta Biomater 2009;5(6):2063–2071. [PubMed: 19362063]
41. Salmoria GV, Klauss P, Paggi RA, Kanis LA, Lago A. Structure and mechanical properties of cellulose based scaffolds fabricated by selective laser sintering. Polym Test 2009;28:648–652.

42. Shishkovsky IV, Volova LT, Kuznetsov MV, Morozov YG, Parkin IP. Porous biocompatible implants and tissue scaffolds synthesized by selective laser sintering from Ti and NiTi. J Mater Chem 2008;18(12):1309–1317.
43. Zhang H, Hao L, Savalani MM, Harris RA, Di Silvio L, Tanner KE. *In vitro* biocompatibility of hydroxyapatite-reinforced polymeric composites manufactured by selective laser sintering. J Biomed Mater Res 2009;91A(4):1018–1027.
44. von Wilmowsky C, Vairaktaris E, Pohle D, et al. Effects of bioactive glass and b-TCP containing three-dimensional laser sintered polyetheretherketone composites on osteoblasts *in vitro*. J Biomed Mater Res A 2008;87A(4):896–902. [PubMed: 18228252]
45. Hao L, Savalani MM, Zhang Y, Tanner KE, Harris RA. Selective laser sintering of hydroxyapatite reinforced polyethylene composites for bioactive implants and tissue scaffold development. Proc Inst Mech Eng H 2006;220(4):521–531. [PubMed: 16808068]
46. Shishkovsky I, Yadroitsev I, Bertrand P, Smurov I. Alumina–zirconium ceramics synthesis by selective laser sintering/melting. Appl Surf Sci 2007;254(4):966–970.
47. Shabalovskaya SA. On the nature of the biocompatibility and on medical applications of NiTi shape memory and superelastic alloys. Biomed Mater Eng 1996;6(4):267–289. [PubMed: 8980835]
48. Eliades T, Eliades G, Athanasion AE, Bradley TG. Surface characterization of retrieved NiTi orthodontic archwires. Eur J Orthod 2000;22(3):317–326. [PubMed: 10920564]
49. Rimell JT, Marquis PM. Selective laser sintering of ultra high molecular weight polyethylene for clinical applications. J Biomed Mater Res 2000;53(4):414–420. [PubMed: 10898883]
50. Schmidt M, Pohle D, Rechtenwald T. Selective laser sintering of PEEK. CIRP Ann 2007;56(1): 205–208.
51. Srinivasan R. Ablation of polymers and biological tissue by ultraviolet-lasers. Science 1986;234(4776):559–565. [PubMed: 3764428]
52. Snakenborg D, Klank H, Kutter JP. Microstructure fabrication with a CO_2 laser system. J Micromech Microeng 2004;14(2):182–189.
53. Miller PR, Aggarwal R, Doraiswamy A, Lin YJ, Lee YS, Narayan RJ. Laser micromachining for biomedical applications. JOM 2009;61(9):35–40.
54. Korte F, Nolte S, Chichkov BN, et al. Far-field and near-field material processing with femtosecond laser pulses. Appl Phys A 1999;69:S7–S11.
55. Schmidt V, Kuna L, Satzinger V, Jakopic G, Leising G. Two-photon 3D lithography: A versatile fabrication method for complex 3D shapes and optical interconnects within the scope of innovate industrial applications. J Laser Micro/Nanoeng 2007;2(3):170–177.
56. Gattass RR, Mazur E. Femtosecond laser micromachining in transparent materials. Nat Photon 2008;2(4):219–225.
57. Joglekar AP, Liu H, Spooner GJ, Meyhofer E, Mourou G, Hunt AJ. A study of the deterministic character of optical damage by femtosecond laser pulses and applications to nanomachining. Appl Phys B 2003;77(1):25–30.
58. Vogel A, Venugopalan V. Mechanisms of pulsed laser ablation of biological tissues. Chem Rev 2003;103(2):577–644. [PubMed: 12580643]
59. Chichkov BN, Momma C, Nolte S, von Alvensleben F, Tunnermann A. Femtosecond, picosecond and nanosecond laser ablation of solids. Appl Phys A 1996;63(2):109–115.
60. Preuss S, Demchuk A, Stuke M. Subpicosecond UV laser-ablation of metals. Appl Phys A Mater Sci Process 1995;61(1):33–37.
61. Stoeckel D, Bonsignore C, Duda S. A survey of stent designs. Minim Invasive Ther Allied Technol 2002;11(4):137–147. [PubMed: 16754063]
62. Stoeckel D, Pelton A, Duerig T. Self-expanding nitinol stents: material and design considerations. Eur Radiol 2004;14(2):292–301. [PubMed: 12955452]
63. Momma C, Knop U, Nolte S. Laser cutting of slotted tube coronary stents – state-of-the-art and future developments. Prog Biomed Res 1999:39–44.

64. Grabow N, Schlun M, Sternberg K, Hakansson N, Kramer S, Schmitz KP. Mechanical properties of laser cut poly(l-lactide) micro-specimens: Implications for stent design, manufacture, and sterilization. J Biomech Eng Trans 2005;127(1):25–31.

65. Lannutti J, Reneker D, Ma T, Tomasko D, Farson DF. Electrospinning for tissue engineering scaffolds. Mater Sci Eng C 2007;27(3):504–509.

66. Duncan AC, Rouais F, Lazare S, Bordenave L, Baquey C. Effect of laser modified surface microtopochemistry on endothelial cell growth. Colloid Surf B 2007;54(2):150–159.

67. Patz TM, Doraiswamy A, Narayan RJ, Modi R, Chrisey DB. Two-dimensional differential adherence and alignment of C2C12 myoblasts. Mater Sci Eng B 2005;123(3):242–247.

68. Doraiswamy A, Patz T, Narayan RJ, et al. Two-dimensional differential adherence of neuroblasts in laser micromachined CAD/CAM agarose channels. Appl Surf Sci 2006;252(13):4748–4753.

69. Choi HW, Johnson JK, Nam J, Farson RF, Lannutti J. Structuring electrospun polycaprolactone nanofiber tissue scaffolds by femtosecond laser ablation. J Laser Appl 2007;19(4):225–231.

70. Applegate RW, Schafer DN, Amir W, et al. Optically integrated microfluidic systems for cellular characterization and manipulation. J Opt A 2007;9(8):S122–S128.

71. Vazquez RM, Osellame R, Cretich M, et al. Optical sensing in microfluidic lab-on-a-chip by femtosecond-laser-written waveguides. Anal Bioanal Chem 2009;393(4):1209–1216. [PubMed: 18839156]

72. Sugioka K, Hanada Y, Midorikawa K. 3D integration of microcomponents in a single glass chip by femtosecond laser direct writing for biochemical analysis. Appl Surf Sci 2007;253(15):6595–6598.

73. Hanada Y, Sugioka K, Kawano H, Ishikawa IS, Miyawaki A, Midorikawa K. Nano-aquarium for dynamic observation of living cells fabricated by femtosecond laser direct writing of photostructurable glass. Biomed Microdevices 2008;10(3):403–410. [PubMed: 18080201]

74. Ancona A, Roeser F, Rademaker K, Limpert J, Nolte S, Tuennermann A. High speed laser drilling of metals using a high repetition rate, high average power ultrafast fiber CPA system. Opt Express 2008;16(12):8958–8968. [PubMed: 18545607]

75. Ancona A, Nodop D, Limpert J, Nolte S, Tuennermann A. Microdrilling of metals with an inexpensive and compact ultra-short-pulse fiber amplified microchip laser. Appl Phys A 2009;94(1):19–24.

76. Pique A, Chrisey DB, Auyeung RCY, et al. A novel laser transfer process for direct writing of electronic and sensor materials. Appl Phys A 1999;69:S279–S284.

77. Chrisey DB, Pique A, Fitz-Gerald J, et al. New approach to laser direct writing active and passive mesoscopic circuit elements. Appl Surf Sci 2000;154:593–600.

78. Ringeisen BR, Callahan J, Wu PK, et al. Novel laser-based deposition of active protein thin films. Langmuir 2001;17(11):3472–3479.

79. Ringeisen BR, Chrisey DB, Pique A, et al. Generation of mesoscopic patterns of viable *Escherichia coli* by ambient laser transfer. Biomaterials 2002;23(1):161–166. [PubMed: 11762834]

80. Wu PK, Ringeisen BR, Krizman DB, et al. Laser transfer of biomaterials: matrix-assisted pulsed laser evaporation (MAPLE) and MAPLE direct write. Rev Sci Instrum 2003;74(4):2546–2557.

81. Dinu CZ, Dinca V, Howard J, Chrisey DB. Printing technologies for fabrication of bioactive and regular microarrays of streptavidin. Appl Surf Sci 2007;253(19):8119–8124.

82. Wu PK, Ringeisen BR, Callahan J, et al. The deposition, structure, pattern deposition, and activity of biomaterial thin-films by matrix-assisted pulsed-laser evaporation (MAPLE) and MAPLE direct write. Thin Solid Films 2001;398:607–614.

83. Doraiswamy A, Narayan RJ, Lippert T, et al. Excimer laser forward transfer of mammalian cells using a novel triazene absorbing layer. Appl Surf Sci 2006;252(13):4743–4747.

84. Patz TM, Doraiswamy A, Narayan RJ, et al. Three-dimensional direct writing of B35 neuronal cells. J Biomed Mater Res B 2006;78(1):124–130.

85. Doraiswamy A, Narayan RJ, Harris ML, Qadri SB, Modi R, Chrisey DB. Laser microfabrication of hydroxyapatite-osteoblast-like cell composites. J Biomed Mater Res A 2007;80A(3):635–643. [PubMed: 17051538]

86. Venuvinod, PK.; Ma, W. Rapid Prototyping: Laser-based and Other Technologies. Kluwer Academic Publishers; Dordrecht, The Netherlands: 2004. p. 245-278.

87. Ovsianikov, A.; Passinger, S.; Houbertz, R.; Chichkov, BN. Three dimensional material processing with femtosecond lasers. In: Phipps, CR., editor. Laser Ablation and Its Applications. Springer; NY, USA: 2007. p. 121-157.••Chapter discussing the two-photon polymerization process.

88. Gittard SD, Narayan RJ, Lusk J, et al. Rapid prototyping of scaphoid and lunate bones. Biotechnol J 2009;4(1):129–134. [PubMed: 19156737]

89. Lee JW, Lan PX, Kim B, Lim G, Cho D. 3D scaffold fabrication with PPF/DEF using micro-stereolithography. Microelectron Eng 2007;84(5–8):1702–1705.

90. Lee JW, Ahn G, Kim DS, Cho D. Development of nano- and microscale composite 3D scaffolds using PPF/DEF-HA and micro-stereolithography. Microelectron Eng 2009;86(4–6):1465–1467.

91. Arcaute K, Mann BK, Wicker RB. Stereolithography of three-dimensional bioactive poly(ethylene glycol) constructs with encapsulated cells. Ann Biomed Eng 2006;34(9):1429–1441. [PubMed: 16897421]

92. Subburaj K, Nair C, Rajesh S, Meshram SM, Ravi B. Rapid development of auricular prosthesis using CAD and rapid prototyping technologies. Int J Oral Maxillofac Surg 2007;36(10):938–943. [PubMed: 17822875]

93. Singare S, Dichen L, Bingheng L, Yanpu L, Zhenyu G, Yaxiong L. Design and fabrication of custom mandible titanium tray based on rapid prototyping. Med Eng Phys 2004;26(8):671–676. [PubMed: 15471695]

94. Singare S, Dichen L, Bingheng L, Zhenyu G, Yaxiong L. Customized design and manufacturing of chin implant based on rapid prototyping. Rapid Prototyping J 2005;11(2):113–118.

95. Singare S, Lian Q, Wang WP, et al. Rapid prototyping assisted surgery planning and custom implant design. Rapid Prototyping J 2009;15(1):19–23.

96. D'Urso PS, Earwaker WJ, Barker TM, et al. Custom cranioplasty using stereolithography and acrylic. Br J Plast Surg 2000;53(3):200–204. [PubMed: 10738323]

97. Wurm G, Tomancok B, Holl K, Trenkler J. Prospective study on cranioplasty with individual carbon fiber reinforced polymere (CFRP) implants produced by means of stereolithography. Surg Neurol 2004;62(6):510–521. [PubMed: 15576119]

98. Lee S, Wu C, Lee S, Chen P. Cranioplasty using polymethyl methacrylate prostheses. J Clin Neurosci 2009;16(1):56–63. [PubMed: 19046734]

99. Staffa G, Nataloni A, Compagnone C, Servadei F. Custom made cranioplasty prostheses in porous hydroxy-apatite using 3D design techniques: 7 years experience in 25 patients. Acta Neurochir (Wien) 2007;149(2):161–170. [PubMed: 17242849]

100. Narayan R. Two photon polymerization: An emerging method for rapid prototyping of ceramic-polymer hybrid materials for medical applications. Am Ceram Soc Bull 2009;88(5):20–25.

101. Doraiswamy A, Jin C, Narayan RJ, et al. Two photon induced polymerization of organic-inorganic hybrid biomaterials for microstructured medical devices. Acta Biomater 2006;2(3): 267–275. [PubMed: 16701886]

102. Serbin J, Egbert A, Ostendorf A, et al. Femtosecond laser-induced two-photon polymerization of inorganic-organic hybrid materials for applications in photonics. Opt Lett 2003;28(5):301–303. [PubMed: 12659425]

103. Ovsianikov A, Chichkov B, Adunka O, Pillsbury H, Doraiswamy A, Narayan RJ. Rapid prototyping of ossicular replacement prostheses. Appl Surf Sci 2007;253(15):6603–6607.

104. Lee KS, Kim RH, Yang DY, Park SH. Advances in 3D nano/microfabrication using two-photon initiated polymerization. Prog Polym Sci 2008;33(6):631–681.

105. Lim TW, Son Y, Yang DY, Kong HJ, Lee KS, Park SH. Highly effective three-dimensional large-scale microfabrication using a continuous scanning method. Appl Phy A 2008;92(3):541–545.

106. Hemker KJ, Sharpe WN Jr. Microscale characterization of mechanical properties. Ann Rev Mater Res 2007;37:93–126.

107. Ovsianikov A, Chichkov B, Mente P, Monteiro-Riviere NA, Doraiswamy A, Narayan RJ. Two photon polymerization of polymer-ceramic hybrid materials for transdermal drug delivery. Int J Appl Ceram Technol 2007;4(1):22–29.

108. Ovsianikov A, Ostendorf A, Chichkov BN. Three-dimensional photofabrication with femtosecond lasers for applications in photonics and biomedicine. Appl Surf Sci 2007;253(15): 6599–6602.

109. Gittard SD, Ovsianikov A, Monteiro-Riviere NA, et al. Fabrication of polymer microneedles using a two-photon polymerization and micromolding process. J Diabetes Sci Technol 2009;3(2): 304–311. [PubMed: 20144361]

110. Brown MB, Martin GP, Jones SA, Akomeah FK. Dermal and transdermal drug delivery systems: current and future prospects. Drug Deliv 2006;13(3):175–187. [PubMed: 16556569]

111. Gill HS, Denson DD, Burris BA, Prausnitz MR. Effect of microneedle design on pain in human volunteers. Clin J Pain 2008;24(7):585–594. [PubMed: 18716497]

112. Narayan RJ, Jin CM, Doraiswamy A, et al. Laser processing of advanced bioceramics. Adv Eng Mater 2005;7(12):1083–1098.

113. Tayalia P, Mendonca CR, Baldacchini T, Mooney DJ, Mazur E. 3D cell-migration studies using two-photon engineered polymer scaffolds. Adv Mater 2008;20(23):4494–4498.

114. Schlie S, Ngezahayo A, Ovsianikov A, et al. Three-dimensional cell growth on structures fabricated from ORMOCER® by two-photon polymerization technique. J Biomater Appl 2007;22(3):275–287. [PubMed: 17494962]

115. Claeyssens F, Hasan EA, Gaidukeviciute A, et al. Three-dimensional biodegradable structures fabricated by two-photon polymerization. Langmuir 2009;25(5):3219–3223. [PubMed: 19437724]

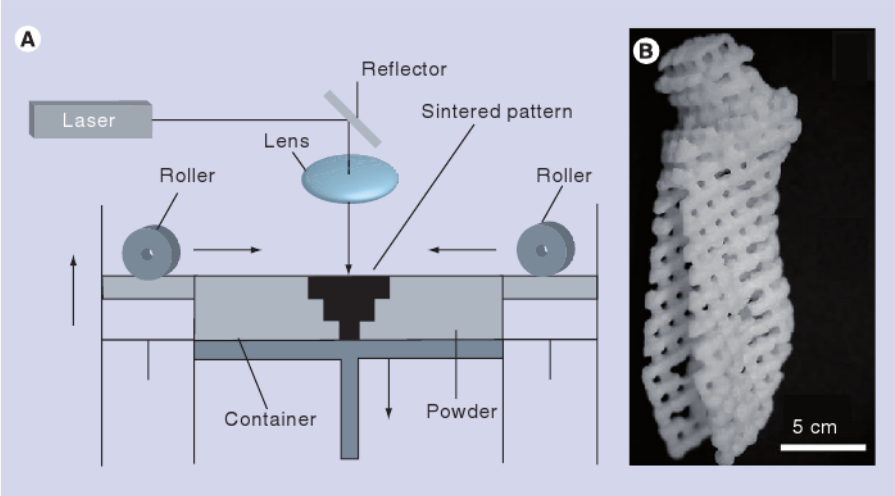

Figure 1. Selective laser sintering process

(A) Schematic of selective laser sintering process. **(B)** Poly(caprolactone) tissue-engineering scaffold in the shape of a human condyle; this structure was fabricated using selective laser sintering.

(A) Reprinted from [21] with permission from Elsevier © 1999.

(B) Reprinted from [39] with permission from ASME.

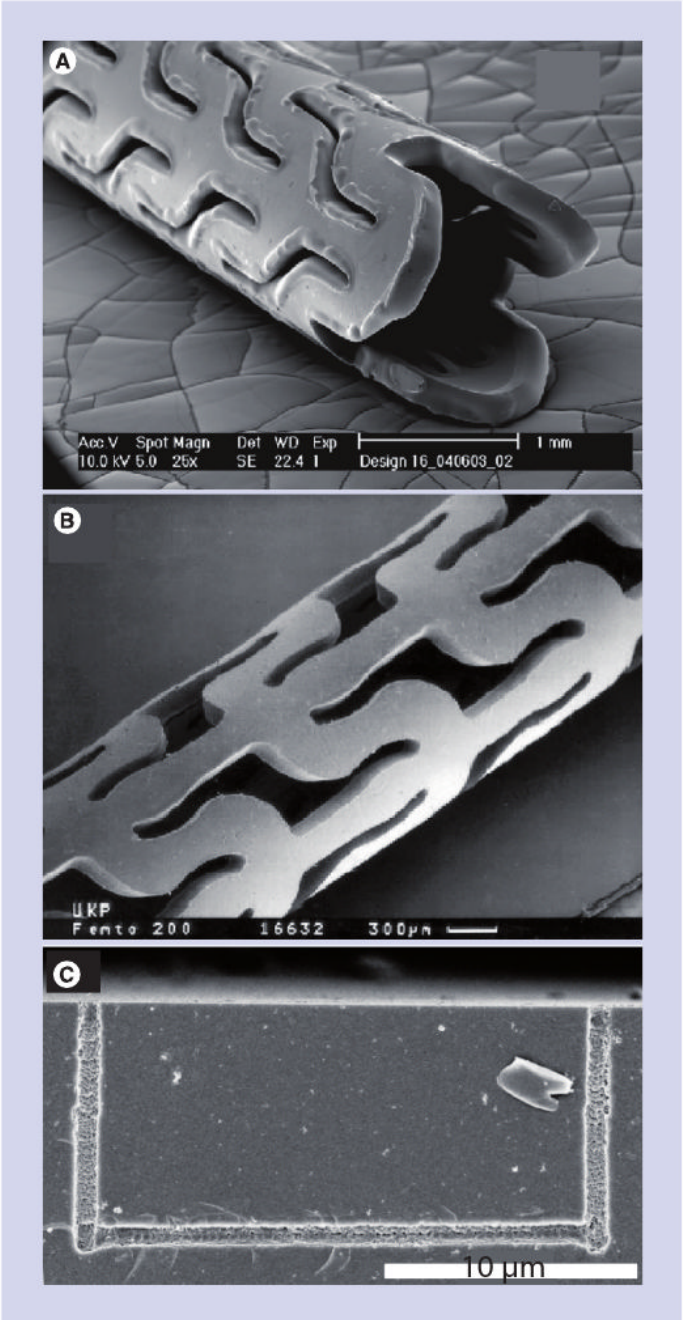

Figure 2. Laser machining process

(A) Poly(L-lactide) stent machined using a continuous wave CO_2 laser. **(B)** Poly(L-lactide) stent machined using a femtosecond laser. **(C)** Glass microfluidic device containing a nano-scale channel machined on the interior of the structure using a femtosecond laser.

(A) Reprinted from [64] with permission from ASME.

(B) Reprinted from [55] with kind permission of Springer, Science+Business Media © 1999.

(C) Reprinted with permission from [1]. © 2005 American Chemical Society.

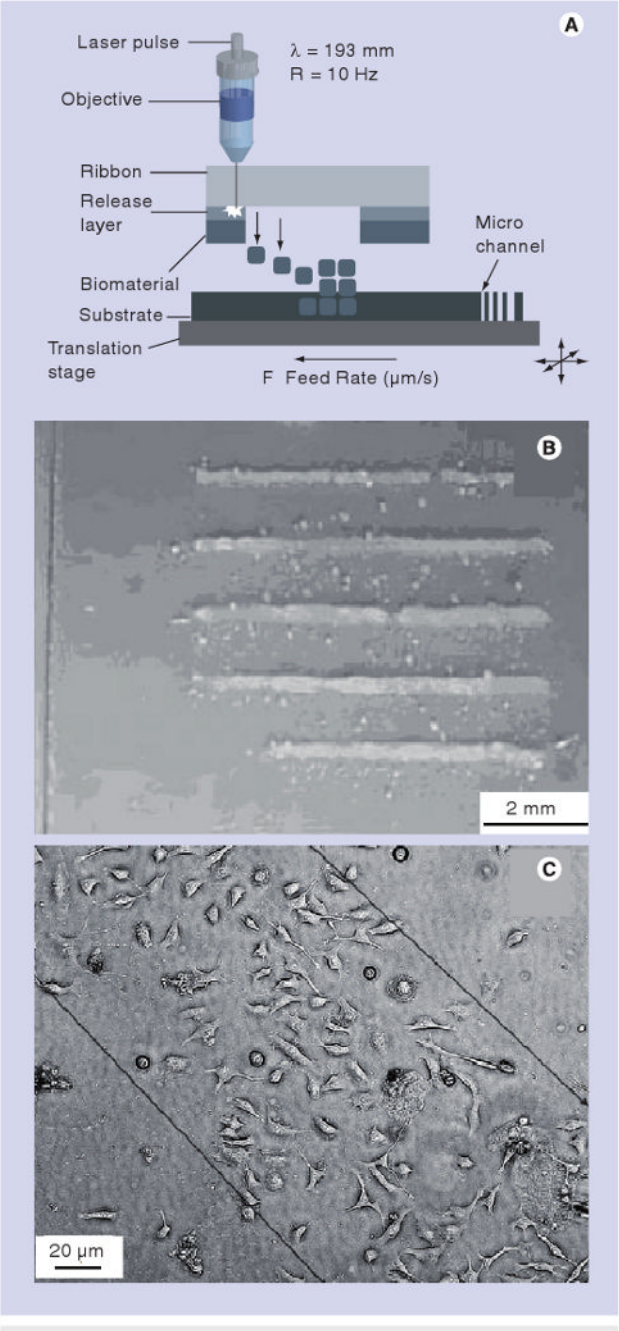

Figure 3. Matrix-assisted pulsed-laser evaporation direct write process

(A) Schematic of the matrix-assisted pulsed-laser evaporation direct write process. **(B)** Patterns of hydroxyapatite on borosilicate glass deposited by matrix-assisted pulsed-laser evaporation direct write. **(C)** Line of B35 neuroblast cells deposited by matrix-assisted pulsed-laser evaporation direct write.

(A) Reprinted from [3], with permission from Elsevier © 2008.

(B) Reprinted from [85] with permission from John Wiley and Sons.

(C) Reprinted from [83] with permission from Elsevier © 2006.

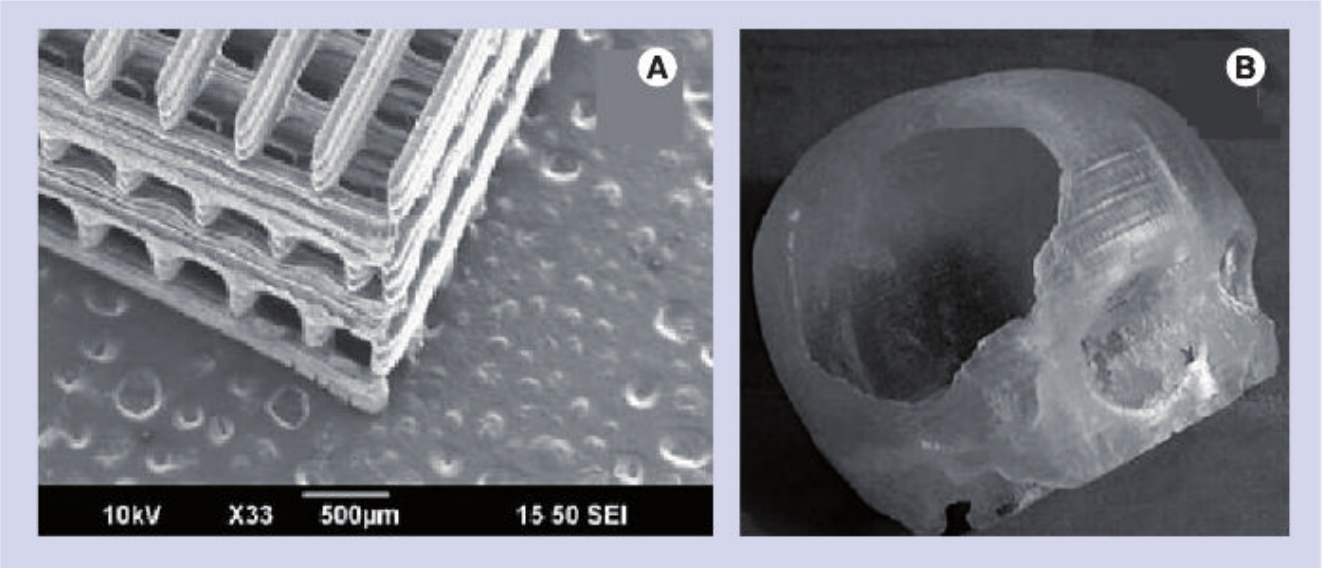

Figure 4. Stereolithography process

(A) Composite PPF/DEF-hydroxyapatite tissue-engineering scaffold fabricated by stereolithography. **(B)** Reconstruction of a human skull defect produced by stereolithography of an epoxy thermosetting polymer. The model was then used to mold a hydroxyapatite prosthesis.

(A) Reprinted from [90] with permission from Elsevier © 2009.

(B) Reprinted from [99] with kind permission of Springer © 2007.

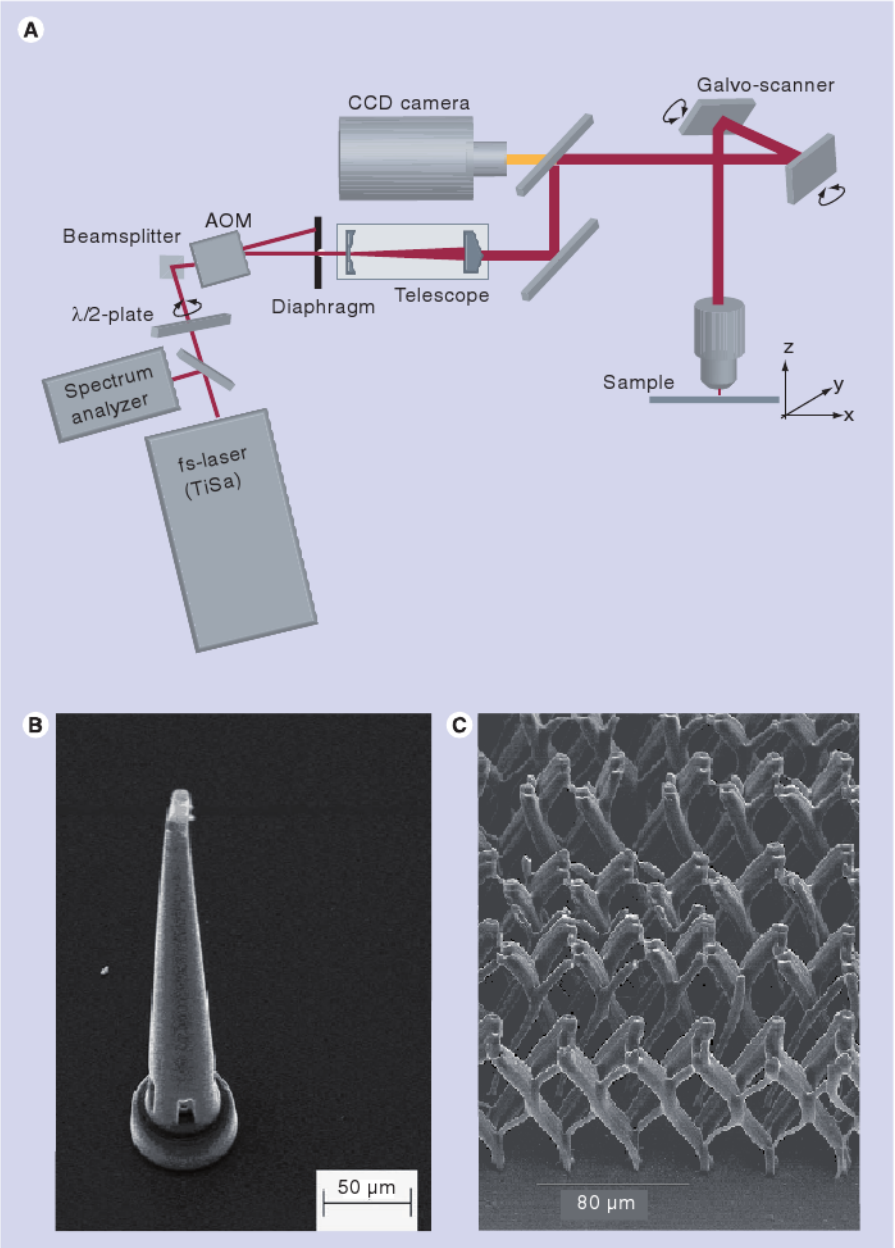

Figure 5. Two-photon polymerization process

(A) Schematic of a two-photon polymerization system. **(B)** Ormocer® microneedle fabricated by two-photon polymerization. **(C)** Micrometer-scale Ormocer® tissue-engineering scaffold with varying pore sizes on different axes.

ADM: Acousto–optical modulator; CCD: Charge coupled device; TiSa: Titanium sapphire.

(A) & **(B)** Reprinted from [101] with permission from Elsevier © 2006.

(C) Reprinted from [110] with permission from Elsevier © 2007.

Table 1

Comparison of laser direct writing processes

Technique	Laser type	Resoulation	Applications	Compatible materials	Limitation
Selective laser sintering/melting	CW, LP	50 μm	Prosthetics Tissue engineering	Ceramics Polymers Metals	Powder precursor High temperature Layered fabrication
Micro-laser sintering	LP	20 μm	Prosthetics	Ceramics Metals	Powder precursor High temperature Layered fabrication
Laser machining	CW, EX, LP, SP, USP	15 nm	Microfluidics Stents Tissue engineering	Ceramics Polymers Metals	Top-down
Matrix-assisted pulsed-laser evaporation direct write	EX	10 μm	Microelectronics Chemical sensors Tissue engineering	Polymers Metals Ceramics Biomolecules	Multiple processing parameters Layered fabrication
Stereolithography	CW	1 μm	Prosthetics Tissue engineering	Polymers Ceramic composites Biomolecule composites	Photopolymerization Layered fabrication
Two-photon polymerization	USP	<100 nm	Drug deliveryprosthetics Tissue engineering	Polymers Ceramic composites	Photopolymerization

CW: Continuous wave (e.g., CO_2, Ar^+); EX: Excimer (e.g., ArF, KrF); LP: Long pulse (ms – 100 ps); SP: Short pulse (<100 ps); USP: Ultra-short pulse (fs).